PCCP

Accepted Manuscript

ROYAL SOCIETY OF CHEMISTRY

www.rsc.org/pccp

Defect Relaxation Insight in Metastable ZnO Reflected by Unique Luminescence and Raman Evolutions

Haibo Zeng[1,2]*, Xue Ning[1,2], Xiaoming Li[1,2]

[1]*State Key Laboratory of Mechanics and Control of Mechanical Structures & College of Materials Science and Technology, Nanjing University of Aeronautics and Astronautics, Nanjing, China*

[2]*Institute of Optoelectronics & Nanomaterials, College of Material Science and Engineering, Nanjing University of Science and Technology, Nanjing210094, China*

Abstract

Defects play a crucial role in semiconductors, but a facile method to observe defect variation inside semiconductors is still absent. Here, we report on a defect relaxation insight in metastable ZnO nanoparticles, which are prepared by nonequilibrium laser ablation in liquid media, reflected by the Raman vibrations of surface optical (SO) and volume phonons, as well as by the evolution of luminescence. During the annealing process, the SO and volume phonon modes exhibit strong incompatibility and a unique "intermission" period at the temperature from 300 ^{o}C to 400 ^{o}C, in which both the vibrations are completely suppressed on the Raman spectra. Combining with the corresponding defects-related photoluminescence spectra, it is demonstrated that there exists a delay between the reconstruction of the interfacial defects and annihilation of other intrinsic defects, including interstitial zinc and oxygen vacancy, in the relaxation process, and that the sequence of different defects of ZnO in the instability is interfacial defect, interstitial zinc, and then oxygen vacancy. Such defect relaxation will deepen our understanding in some properties of semiconducting nanomaterials, including luminescence, photocatalysis, electronic transport, sensors and others.

Introduction

The relaxation of disordered structure and lattice defects in crystal governs the physical properties of a solid (especially, a nanocrystal material), which has been investigated for a long time in the field of physics.[1] As an important wide-band-gap semiconductor, nanostructured ZnO has attracted considerable interest due to its potential applications in electronic and optical devices, especially, in optoelectronics, such as, the ultraviolet (UV)/blue lasing media.[2] Due to the co-existing properties of semiconductor and metal, the Zn-ZnO core-shell nanostructures have attracted some interest, but the attentions are mostly paid on their structures. These applications are intensively affected by the state of the intrinsic defects, for instance, interstitial zinc and oxygen vacancy.[3] Though the development and defects related visible emission have developed forward step by step and interesting and convincing results were obtained,[4-7] there still exist extensive controversies in both the dominant defects and the mechanisms of the visible emissions in ZnO.[3, 8-12] As we know, when the dimensions are reduced to the nanoscale, the interfacial defects of material will become crucial, and induce some Raman-forbidden phonon-vibration modes, such as, surface optical (SO) phonon mode, due to impurity, imperfections, or valence band mixing of nano-structures, which can be used as the fingerprint or indication of the disorder degree of atomic arrangement in nanoscale.[13-15]

Laser ablation in a liquid medium is of particular interest, due to its extreme nonequilibrium feature, which allows synthesis of novel metastable phases of materials.[16-19] The obtained products usually possess high-concentration defects, which provide us the suitable samples to investigate the thermal stability and relaxation of defects. In this work, we study the thermal stability and relaxation of the interfacial and intrinsic defects in Zn/ZnO core-shell nanoparticles, synthesized by pulsed-laser ablation in a liquid medium, using laser Raman scattering and photoluminescence (PL) spectra.

Experiment

The laser ablation of a zinc target was performed in an aqueous solution with surfactant sodium dodecyl sulfate (SDS, 99.5%), as previously reported in details by our group and others.[19-22] Briefly, a zinc plate (99.99%) was fixed on a bracket in a glass vessel filled with 10 mL 0.05 M SDS (99.5%) aqueous solution, which was continuously stirred. The plate was located at 4mm from the solution surface in the solution, and then was ablated for 30 min by the first harmonic of a Nd:YAG pulsed laser (wavelength 1064 nm, frequency 10 Hz, pulse duration 10 ns) with the power of 70 mJ/pluse, and the spot size of about 2 mm in diameter. After ablation, all of the colloidal suspensions were centrifuged at 14000 rpm, rinsed with ethanol for several times to remove the covered surfactant, and dried at room temperature before characterization, further annealing treatment, Raman scattering and PL measurements.

Characterizations

X-ray diffraction (XRD) patterns were recorded on a multipurpose XRD system D8 Advance from Bruker with a $Cu_{K\alpha}$ radiation. TEM and HRTEM images were recorded on FEI Tecnai F30 S-TWIN. Raman spectra were measured on a JY HR800 tool with laser excitation of 514.5 nm. Photoluminescence (PL) spectra were measured with a Varian Cary Eclipse instrument.

Results

The typical characterization and their evolution with anneal were presented in Figure 1. As shown in Fig. 1 A, two sets of XRD diffraction peaks corresponding to metal Zn and wurtzite ZnO crystals were observed in X-ray diffraction (XRD) pattern of the as-synthesized samples. With annealing temperature increasing, the Zn diffraction peaks decrease and the ZnO diffraction peaks increase. The sharp change occurs when the temperature is above 300 ^{o}C. TEM image of the primal sample revealed that it is consist of nearly spherical nanoparticles with average diameter about 20 nm (Fig. 1 B). HRTEM shows that the particles are of core-shell structure with zinc core and ZnO shell of 6 nm in typical thickness (see Fig. 1C). The Zn core is well crystallized. The ZnO shell, however, is composed of a lot of ultra-fine nanocrystals with different lattice orientations (see circular areas marked in Fig. 1 D), and a great deal of disorderly arranged areas located in the boundaries among these nanocrystals, which are expected to intensively influence its properties and also provide us a

good model material to study the thermal stability and defect relaxation behaviors. The 300 ^{o}C annealed sample has been completely oxidized, showing well monocrystalline in Fig. 1 E, which is agreeable to the XRD evolution.

The formation of such core-shell structured Zn/ZnO nanparticles can be attributed to the competition between aqueous oxidation and surfactant protection of Zn clusters during the pulsed-laser-induced reactive quenching process, which are produced in the high-temperature and high-pressure zinc plasma on the solid-liquid interface quickly after the interaction between pulsed laser and the metal target.[21] It is just due to the highly nonequilibrium character, including the plasma extreme conditions and the ultra-rapid reactive quenching, that we can obtain such nanoparticles with special microstructure, and hence unique properties.

Fig. 2 shows the Raman scattering spectrum of the as-prepared Zn/ZnO nanoparticles using a 514.5 nm laser as excitation source. In the as-prepared nanoparticles, all of the normal volume phonon vibration modes of ZnO[23] hardly emerge, but an abnormal and dominant Raman peak at about 560 cm^{-1} is observed, which is between the transverse optical (TO) and longitudinal optical (LO) phonon modes, as shown in Fig. 2 A. Such abnormal Raman peak shows dependence on media surrounding the particles (red-shift with increase of dielectric constant) and obvious confinement effect (blue-shift with decrease of shell thickness) as our previous report. As for the origination of the abnormal Raman mode, its frequency location, medium dependence, and confinement effect are as similar to those of the surface optical (SO) phonon vibration modes of previously reported ZnS nanowires and SnO_2 nanocrystals.[13-15] Thereby, this abnormal Raman peak can be attributed to the SO phonon vibration mode of ZnO induced by a great deal of interfacial defects, such as disorderly arranged atoms, grain boundaries (as shown in Fig. 1 D), and just be the result of the loss of long-range periodicity (breakdown of symmetry) in the ZnO shell. Therefore, the SO phonon mode can be used as a measurement of the disordered degree in this nanostructure,[13, 15] while the volume phonon vibration modes (such as, TO mode at 380 cm^{-1}) can be used as an indication of the ordered degree.

More interestingly, such abnormal phonon mode exhibits very high sensitivity to

annealing conditions, as illustrated in Fig. 2. It obviously decreased with the annealing. Especially, when the annealing temperature was above 300 ^{o}C, the weakening rate was greatly accelerated, even induced the annihilating at the conditions of 300 ^{o}C 3 hours. After that, the complete quenching phenomenon was maintained till the high temperature annealing-induce the occurrence of the normal volume phonon. When annealing at 500 ^{o}C or higher, the volume phonon modes, which are well coincided with the reported volume phonon modes of nanostructured ZnO,[23] appear and increase with temperature. During this Raman evolution process with annealing, at a mid-temperature range from 300 ^{o}C 3 h to 400 ^{o}C, both abnormal phonon modes and the volume phonon modes are all completely suppressed, exhibiting an "intermission" period of phonon vibration, which is a very vagarious and unexpected phenomenon. What is the physical meaning of such strange "intermission" in the aspects of symmetry or ordering degree evolvement during the annealing process?

Fig. 3 shows the corresponding PL evolution with annealing. For the as-synthesized sample, a strong violet emission peak centered at 425 nm (2.92 eV) is observed. Subsequent annealing induce decrease of the violet emission, accompanied with appearance and increase of the conventional green emission at 510 nm, with rise in the temperature up to 400 ^{o}C (3 h), at which the violet emission disappear and the characteristic UV emission at 380 nm appears in addition to the green one. Further increasing annealing temperature results in rise in the intensity ratio of UV/green emissions. In our previous reports, the violet and green emissions are found to be associated with two different electron paramagnetic resonance signals g = 2.05 and g = 1.9652, respectively.[24] The latter is well coincided with the widely reported oxygen vacancy in ZnO.[5, 10, 25] Based on the accordance of the emission energy of the violet PL with the calculated defect level of the interstitial zinc by full-potential linear muffin-tin orbital,[9] the violet emission can be attributed to the radiative transition of electrons from the local interstitial zinc defect level to the valence band.

Discussions

Based on the evolution of these two characteristic modes with annealing shown in Fig. 3,

the thermal relaxation of the disorder degree with annealing can be measured by intensity evolution of the two phonon modes, as seen in Fig. 4, which can be divided into three regions corresponding with different annealing temperatures. On the one hand, region Ⅱ well presents the "intermission" of the relaxation of disorder degree. On the other hand, in regions □ and III, the disordering-related and ordering-related phonon modes exhibit strong incompatibility. These are completely contrary to what we usually expect, i.e. with the annealing process, the reduction of disorderly arranged atoms should be accompanied by increase of the ordered degree of the lattice, or decrease of SO mode should be accompanied by appearance and increase of TO mode. In fact, this "intermission" and incompatibility reflect that there exists some factor which induces the complete suppression of the volume phonon vibration modes in region I and □.

As we know, the SO mode comes from the interfacial defects at the grain boundaries in the ZnO shell, but the volume modes come from the phonon vibrations of the inner lattice of the ultra-fine crystal grains in the ZnO shell and reflects the perfect symmetry of ZnO lattice. The complete suppression indicates the great destruction of the normal symmetry of inner ZnO lattice, which should be not related to the interfacial defects, and may be induced by intrinsic defects such as vacancy and interstitial defects. If in this case, the "intermission" may be accompanied with strong defect emissions in the photoluminescence (PL) spectra.

In order to find the correlation between the evolutions of the defect emissions and that of the phonon vibrations, the intensity evolution of the defect emissions is also divided into three regions as shown in Fig. 4. It is found that in region I, there exist strong emission from interstitial zinc and weak oxygen vacancy emission; in region Ⅱ, there co-exist emissions from both interstitial zinc and oxygen vacancy but opposite evolution with temperature; In region III, the interstitial zinc emission has annihilated and the oxygen vacancy emission rapidly quenches with rise in annealing temperature.

The observations above indicate that the strong and dominant SO phonon mode for the as-prepared sample is coordinately induced by the strengthening of the SO phonon vibration due to the high-percentage of interfacial disorderly arranged atoms and by the complete suppression of the volume phonons vibration due to the high-concentration of intrinsic zinc.

The high disordering in the ZnO shell is jointly caused by the greatly abundant interfacial defects and interstitial zinc. In region I, with increase of the annealing temperature, the interfacial disorderly arranged atoms are rapidly reduced by reconstruction, which induces the decrease and disappearance of the SO phonon mode. The interstitial zinc concentration decreases with temperature by occupying lattice position, which thus induces increase of oxygen vacancies, showing opposite evolution with annealing temperature up to 400 ^{o}C (see Fig. 4). It means less interstitial zinc but more oxygen vacancies and the distorted lattice is still maintained during annealing at 300-400 ^{o}C temperature. So, neither SO phonon mode nor volume phonon modes is observed in Raman scattering spectra in region II. Only in region III, with high-temperature annealing, the percentage of oxygen vacancy defects decrease to a low level and the lattice distortion is small enough, leading to the appearance and strengthening of the volume phonon vibrations.

It can thus be deduced that there exist different evolution rates for different kinds of defects, including disorderly arranged atoms in interfacial area, interstitial zinc and oxygen vacancies. The disorderly arranged atoms in interfacial area can easily reconstruct at lower temperature (up to 300 ^{o}C), while the zinc interstitials annihilate at up to 400 ^{o}C and the oxygen vacancies significantly reduce at up to 500 ^{o}C, which demonstrates the difference in the stability of the different defects. The most instable is the interfacial defects, the interstitial zinc is the next and the oxygen vacancy is relatively stable. This should be of great significance for the applications in electronic and optical devices of nanostructured ZnO.

As we known, the point defects will induce the lattice distortion, especially for the interstitial defects, which result in the lattice expansion, and hence destroy the normal symmetry in atomic scale. This effect is infinitesimal in a bulk crystal with equilibrium concentration defects, but will be significant in such ZnO shell with high-concentration defects. It is reasonable that there exists interstitial zinc in ZnO lattices, since the nanoparticles are very quickly formed in the extreme conditions or the high temperature and high pressure zinc plasma, and the subsequent rapid reactive quenching, induced by laser ablation in the liquid media. To further confirm defects-related thermal relaxation analyses above, the normative X-ray diffraction was conducted to study the expected lattice expansion,

using Si (PDF Number 790590) (001) diffraction line as reference line for the calibration of the whole diffraction pattern, as shown in Fig. 5. For the as-synthesized Zn/ZnO core-shell nanoparticles, an obvious shift of $\Delta\theta = 0.045^{o}$ towards small angle is assuredly observed for the ZnO (PDF Number 790206) (100) diffraction peak, although the shift becomes less and blurry after 200 ^{o}C and 400 ^{o}C annealing. This indicates that a slight lattice expansion assuredly exists in the ZnO shell. Excluding the effect of the extraneous impurity, such lattice expansion should be caused by zinc interstitials in ZnO shell. The evolution of the lattice expansion with annealing temperature is well coincided with that of defect analyzed above and PL results.

Summary

In summary, the Zn/ZnO core-shell nanoparticles with novel metastable properties can be synthesized by pulsed-laser-induced reactive quenching. There exists an "intermission" period at 300-400 ^{o}C in the thermal relaxation of the disorder degree of the ZnO nanoshell. This is induced by the delay between the annihilations of the interfacial defect and that of the intrinsic defects in the relaxation process. Our results demonstrate the difference in the stability of different kinds of ZnO defects, the most instable is the interfacial defect, the better is the interstitial zinc, and then the oxygen vacancy. Because of the novel metastable properties and unusual defects, the Zn/ZnO core-shell nanoparticles can be expected to greatly expand the electric and optical applications of ZnO nanomaterials.

Acknowledgements:

This work is financially supported by National Basic Research Program of China (grant number 2014CB931700), NSFC (grant number 61222403) and the Priority Academic Program Development of Jiangsu Higher Education Institutions.

References

[1] K. Urita, K. Suenaga, T. Sugai, H. Shinohara, S. Iijima, *Phys. Rev. Lett.* 2005, **94**, 155502.

[2] Z. L. Wang, X. Y. Kong, J. M. Zuo, *Phys. Rev. Lett.* 2003, **91**, 185502.

[3] J. F. Cordaro, Y. Shim, J. E. May, *J. Appl. Phys.* 1986, **60**, 4186-4190.

[4] P. Felbier, J. Yang, J. Theis, R. W. Liptak, A. Wagner, A. Lorke, G. Bacher, U. Kortshagen, *Adv. Funct. Mater.* 2014, **24**, 1988-1993.

[5] H. Kaftelen, K. Ocakoglu, R. Thomann, S. Tu, S. Weber, E. Erdem, *Phys. Rev. B* 2012, **86**, 014113.

[6] A. B. Djurišić, W. C. H. Choy, V. A. L. Roy, Y. H. Leung, C. Y. Kwong, K. W. Cheah, T. K. Gundu Rao, W. K. Chan, H. Fei Lui, C. Surya, *Adv. Funct. Mater.* 2004, **14**, 856-864.

[7] P. Jakes, E. Erdem, *phys. stat. sol. (RRL) - Rapid Res. Lett.* 2011, **5**, 56-58.

[8] G. D. Mahan, *J. Appl. Phys.* 1983, **54**, 3825-3832.

[9] B. Lin, Z. Fu, Y. Jia, *Appl. Phys. Lett.* 2001, **79**, 943-945.

[10] K. Vanheusden, C. H. Seager, W. L. Warren, D. R. Tallant, J. A. Voigt, *Appl. Phys. Lett.* 1996, **68**, 403-405.

[11] S. K. S. Parashar, B. S. Murty, S. Repp, S. Weber, E. Erdem, *J. Appl. Phys.* 2012, **111**, 113712.

[12] A. Janotti, C. G. Van de Walle, *Phys. Rev. B* 2007, **76**, 165202.

[13] Q. Xiong, J. Wang, O. Reese, L. C. Lew Yan Voon, P. C. Eklund, *Nano Lett.* 2004, **4**, 1991-1996.

[14] Z. W. Chen, J. K. L. Lai, C. H. Shek, *Phys. Rev. B* 2004, **70**, 165314.

[15] M. N. Rumyantseva, A. M. Gaskov, N. Rosman, T. Pagnier, J. R. Morante, *Chem. Mater.* 2005, **17**, 893-901.

[16] P. P. Patil, D. M. Phase, S. A. Kulkarni, S. V. Ghaisas, S. K. Kulkarni, S. M. Kanetkar, S. B. Ogale, V. G. Bhide, *Phys. Rev. Lett.* 1987, **58**, 238-241.

[17] S. B. Ogale, P. P. Patil, D. M. Phase, Y. V. Bhandarkar, S. K. Kulkarni, S. Kulkarni, S. V. Ghaisas, S. M. Kanetkar, V. G. Bhide, S. Guha, *Phys. Rev. B* 1987, **36**, 8237-8250.

[18] K. Saito, T. Sakka, Y. H. Ogata, *J. Appl. Phys.* 2003, **94**, 5530-5536.

[19] F. Mafuné, J.-y. Kohno, Y. Takeda, T. Kondow, H. Sawabe, *J. Phys. Chem. B* 2001, **105**, 5114-5120.

[20] H. Usui, Y. Shimizu, T. Sasaki, N. Koshizaki, *J. Phys. Chem. B* 2005, **109**, 120-124.

[21] H. Zeng, W. Cai, Y. Li, J. Hu, P. Liu, *J. Phys. Chem. B* 2005, **109**, 18260-18266.

[22] C.-C. Huang, C.-S. Yeh, C.-J. Ho, *J. Phys. Chem. B* 2004, **108**, 4940-4945.

[23] Y. Zhang, H. Jia, R. Wang, C. Chen, X. Luo, D. Yu, C. Lee, *Appl. Phys. Lett.* 2003, **83**, 4631-4633.

[24] H. Zeng, G. Duan, Y. Li, S. Yang, X. Xu, W. Cai, *Adv. Funct. Mater.* 2010, **20**, 561-572.

[25] E. Erdem, *J. Alloy. Compd.* 2014, **605**, 34-44.

Figure captions

Fig. 1. XRD pattern (A), TEM image (B), HRTEM image (C), and local magnified image (D) of Zn/ZnO nanoparticles obtained by laser ablation of zinc target in 0.05 M SDS aqueous solution with laser power of 70 mJ/pulse. (E) HRTEM image of the 400 ^{o}C annealed nanoparticles.

Fig. 2. Raman scattering spectra of the as-synthesized and annealed samples.

Fig. 3. Photoluminescence spectra of the as-synthesized and annealed samples.

Fig. 4. Relative intensity vs annealing conditions of phonon vibrations from Raman scattering and defect emissions from photoluminescence spectra.

Fig. 5. Normalized XRD patterns of the as-synthesized Zn/ZnO core-shell nanoparticles and with annealing at 200 ^{o}C and 400 ^{o}C using Si (PDF Number 790590) (001) diffraction line for calibration.

Fig. 1

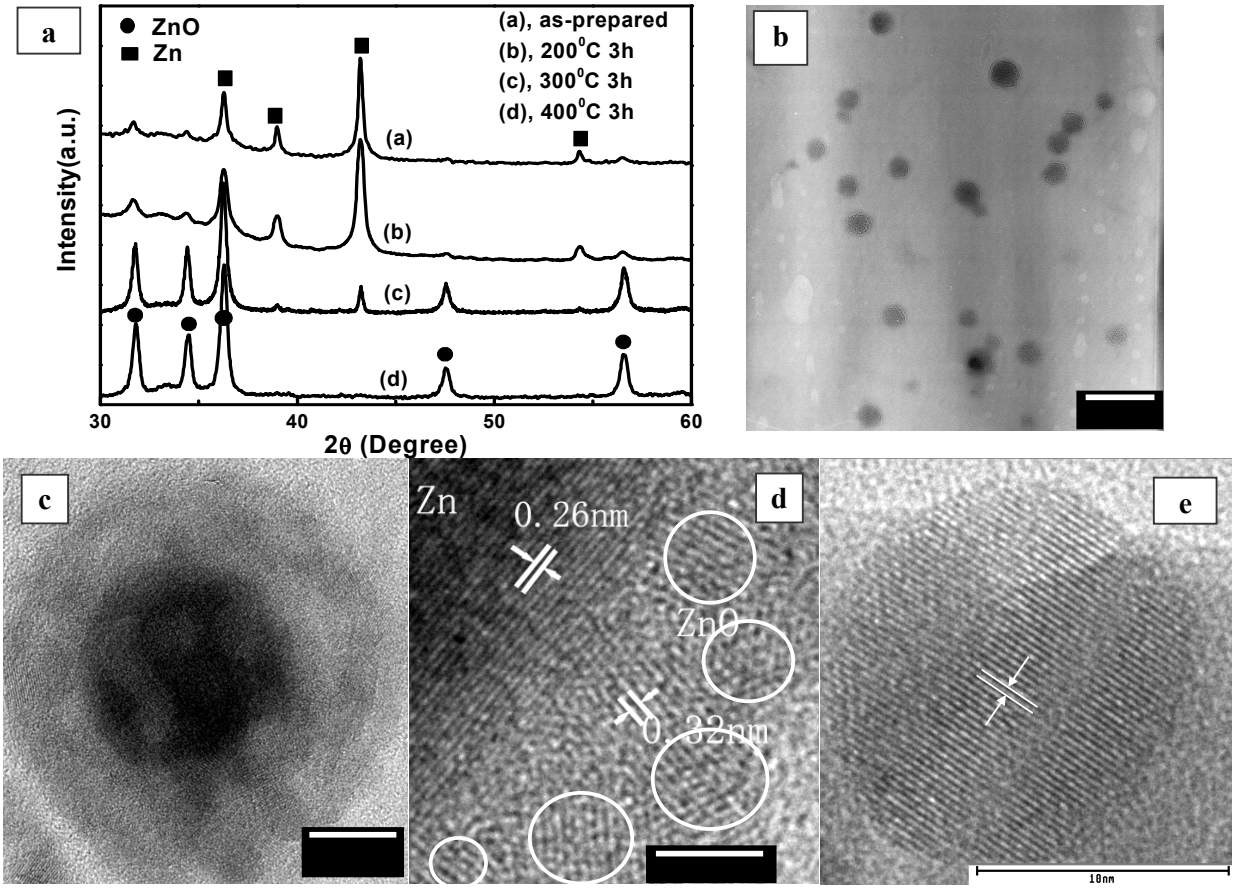

Fig. 2

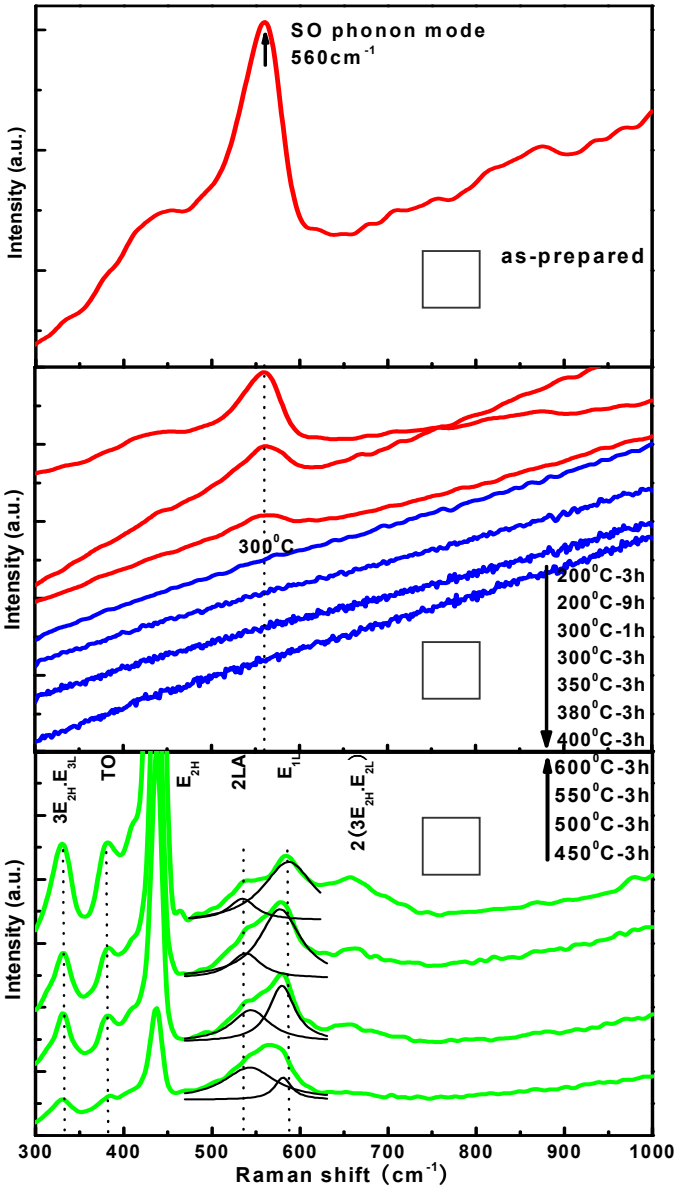

Fig. 3

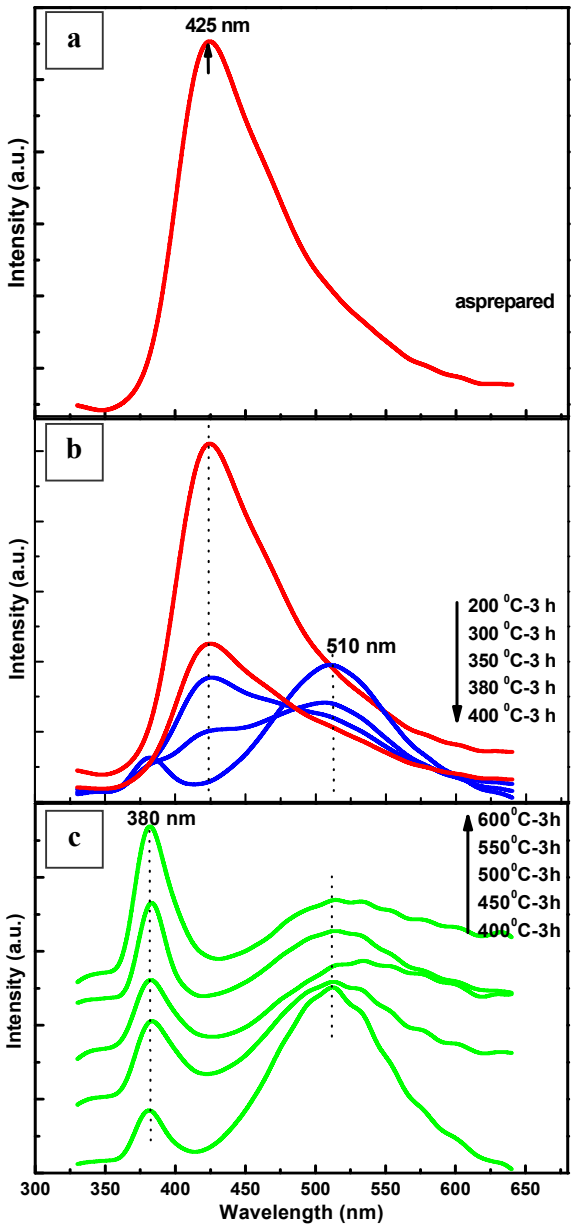

Fig. 4

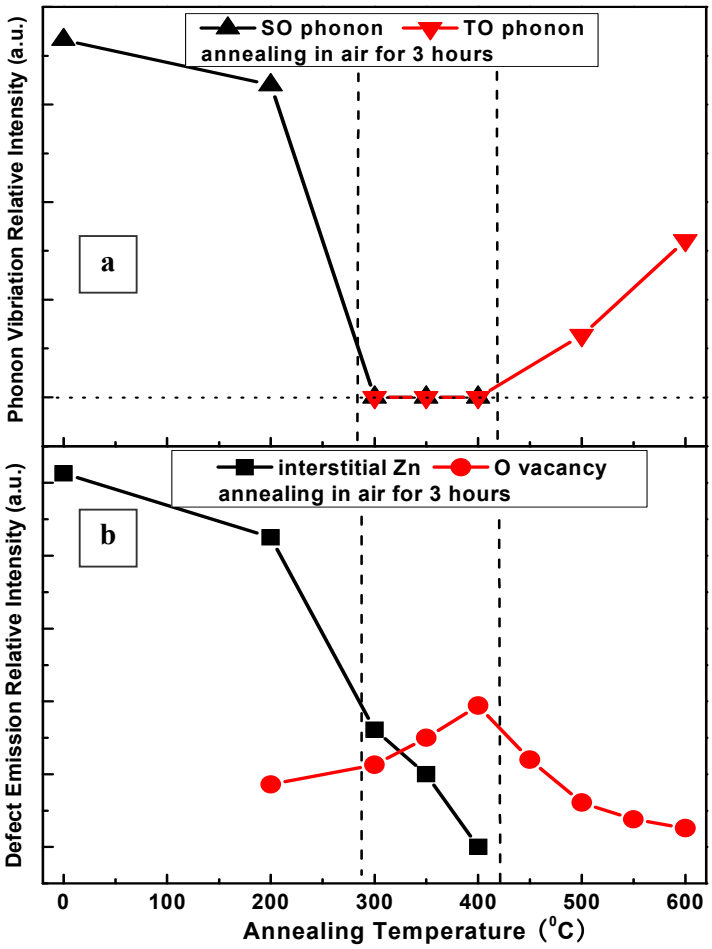

Fig. 5